JOURNAL OF GEOPHYSICAL RESEARCH, VOL. 115, B07104, doi:10.1029/2009JB006445, 2010

Internal structure of the western flank of the Cumbre Vieja volcano, La Palma, Canary Islands, from land magnetotelluric imaging

X. Garcia[1,2] and A. G. Jones[1]

Received 9 March 2009; revised 11 February 2010; accepted 26 February 2010; published 20 July 2010.

[1] Large-scale mass wasting is a natural part of the evolution of volcanic islands, where deformation and indications of flank instability, such as large-scale faulting and seismic and aseismic slip are common. The Cumbre Vieja volcano on the island of La Palma (Canary Islands) provides an ideal setting to address fundamental questions about the structure, evolution and stability of island volcanoes. The island of La Palma is still in a shield-building stage, and it has been postulated that the western side of the island lies over a pre-existing zone of weakness that can nucleate ruptures. We undertook an audiomagnetotelluric (AMT) survey over the proposed unstable western flank to try to image structures that may be associated with the zone of weakness. The magnetotelluric method (MT) is a geophysical technique used to map the presence of fluids or image important structural contrasts. The goals of this study were (1) to delineate the unstable flank, (2) to map the structures underneath and (3) to determine the presence and geometry of fluids. The results show a 1 km thick top resistive layer overlaying an area of reduced resistivity (enhanced conductivity), interpreted as a layer consisting of an alteration zone and also fluids. Our results confirm previous studies that suggested the existence of a western flank lying over collapse debris material and hyaloclastites, and also they allow us to map part of the subaerial southern extent of the Cumbre Nueva units that lie beneath the more recent Cumbre Vieja rocks. In addition, dimensionality analysis maps the rotation of the dike emplacement off ridge, along the western flank in an en echelon fashion.

Citation: Garcia, X., and A. G. Jones (2010), Internal structure of the western flank of the Cumbre Vieja volcano, La Palma, Canary Islands, from land magnetotelluric imaging, *J. Geophys. Res.*, *115*, B07104, doi:10.1029/2009JB006445.

1. Introduction

[2] Large-scale mass wasting is a fundamental process in the evolution of ocean volcanic islands [*Labazuy*, 1996; *Masson et al.*, 2002; *Moore et al.*, 1989]. However, the structures and deformation patterns that result in volcano flank collapses are significantly different between islands formed on fast moving lithosphere (such as Hawaii and Reunion Island) and those formed on slow moving lithosphere (such as Cape Verde and the Canary Islands). A number of mechanical explanations exists for this contrast in behavior, perhaps the simplest of which is that the greater topographic slopes of slow moving plate island volcanoes become catastrophically unstable as soon as they have been weakened by the development of kilometer-scale rupture surfaces. This, in turn, means that pre-existing zones of weakness (such as hyaloclastite or epiclastic breccia deposits), where such ruptures may initially nucleate, might have a more direct control on the geometry of collapse structures in these slow plate volcanoes than in fast plate volcanoes [*Krastel et al.*, 2001; *Mitchell et al.*, 2002]. While both slumping and catastrophic debris avalanches are common features in fast plate volcanoes [*Lipman et al.*, 1988; *Moore et al.*, 1989, 1995], landsliding in slow plate volcanic islands, like the Canary Islands, is dominated by catastrophic debris avalanches, with few indications of slumping.

[3] Several Atlantic volcanic islands in the shield-building stage have been interpreted as showing incipient volcano flank instability that may result in lateral collapse at some time in the future [*Day et al.*, 1999a, 1999b]. In the particular cases of La Palma (Canary Islands) and Fogo (Cape Verde Islands), flank instability appears to be related to the construction of the youngest volcanoes on top of older collapse surfaces that induce topographic-gravitational stresses [*Ward and Day*, 2001].

[4] The island of La Palma (~730 km^2) is one of the youngest islands of the Canarian Archipelago. Recent volcanic activity is concentrated on the southern part of the island, where the Cumbre Vieja volcano (~220 km^2) has been constructed during the past 1 Ma reaching a current elevation

[1]Geophysics Section, School of Cosmic Physics, Dublin Institute for Advanced Studies, Dublin, Ireland.
[2]Now at Unitat de Tecnologia Marina, CSIC, Barcelona, Spain.

0148-0227/10/2009JB006445

of 1898 m above sea level. In Cumbre Vieja, the triple rift geometry typical of volcanic islands has been replaced by a structural configuration that indicates the weakening of the western flank of the volcano. During the most recent eruption near the summit of the Cumbre Vieja in 1949, a west-facing fault system was developed along the crest of the volcano. This has been interpreted as the first surface rupture along a developing zone of deformation and seaward movement [*Day et al.*, 1999b]. Recently, geodetic measurements suggest that the mass may still be creeping seawards at 1–2 cm every few years [*Moss et al.*, 1999], and more recently, *Gonzalez et al.* [2008] suggest a sub-horizontal fault system at 2–3 km depth and an annual creep rate of 12 mm. However, little is known about the geometry of the older structures upon which the younger Cumbre Vieja volcano is resting and growing, since most of our present knowledge and models comes from surface geology observations. The first surface geophysical experiment on the island was a gravity survey undertaken in 2006 by *Camacho et al.* [2009]. Their results show a series of low density anomalies on the western flank interpreted as the presence of debris material from the Cumbre Nueva volcano collapse. In order to understand the factors that control flank instability of young Atlantic volcanoes, it is necessary to gather information about their internal structure using geophysical imaging methods, such as the magnetotelluric (MT) method.

2. AMT Experiment on the Island of La Palma

[5] The MT method is sensitive to bulk and minor properties of a medium. Magnetotelluric data give valuable information regarding the presence of fluids, partial melt or conducting anomalies at shallow levels of the crust and deeper levels of the crust and upper mantle, and also provide first order structure and physico-chemical state (temperature, fluids, melts) of the subsurface. The MT and AMT methods have been used successfully to study various volcanoes, such as the Hawaiian archipelago [*Bartel and Jacobson*, 1987], the island of Tenerife (Canary Islands) by *Pous et al.* [2002] and *Coppo et al.* [2008], to monitor active volcanoes [e.g., *Manzella and Zaja*, 2006; *Ogawa et al.*, 1998; *Matsushima et al.*, 2001; *Aizawa et al.*, 2009], and also in the Aleutians as part of a environmental and hydrological study [*Unsworth et al.*, 2007].

[6] In August 2007, we undertook an AMT survey on the island of La Palma. The overarching goal of this survey was image the internal structure of the island. A secondary goal was to assess the effectiveness of the AMT method for addressing such problems. Given that the island is mostly composed of volcanic material which is very resistive, any appreciable decrease in the internal resistivity would have to be caused by either the presence of an alteration zone consisting of clays, by fluids filling in pores and/or cracks, by partial melt, or any combination of them. Survey design using two-dimensional modeling of the island, based on existing geological models and values of resistivities of basalts and other volcanic materials from previous studies, suggested that the maximum penetration depth between frequencies of 1 and 10 Hz should be ~12 km, sufficient for this study. Given the difficult access of the study area, AMT data at 28 sites were recorded in 8 days of work. These sites were organized in three approximately E-W profiles. The raw time-series were processed using robust processing algorithms [*Jones et al.*, 1989] and the remote reference method was employed using a site located approximately in the middle of the island, north of the three profiles (see Figure 1 for site location).

[7] The high frequency range (10 kHz – 1 kHz) of the AMT data displays the typical erratic behavior within the so-called AMT dead-band [*Garcia and Jones*, 2002]. Therefore, the new wavelet-based algorithm of *Garcia and Jones* [2008] was used to process the data in this high-frequency band. In spite of the fact that the processing algorithm was successful at recovering reliable responses at high frequencies, some sites were severely affected by local topography at these high frequencies, and without a detailed digital terrain elevation model these data were discarded. Nevertheless, the rejected data did not affect the goals of the project.

[8] As mentioned earlier, we organized the data in three E-W profiles labeled NL, ML and SL (Figure 1). Pseudo-sections of the apparent resistivities and phases of these three profiles are plotted in Figure 4, labeled as "OBS" for observed data. The responses are in general of good quality, although some periods and even a whole mode have not been used for the inversion as we describe in a later section. The responses were corrected for galvanic distortion caused by nearby shallow structures using the Groom and Bailey method [*Groom and Bailey*, 1989], as implemented in the "strike" algorithm of *McNeice and Jones* [2001]. Besides correcting for galvanic distortion, this algorithm also performs an analysis of the geo-electric strike. Figure 2 displays the strike angle at three nominal frequencies, showing that a N-S electric strike appears to be the most appropriate to interpret these data using two-dimensional modeling. This agrees with geological models in which a N-S strike for the Cumbre Vieja rift has been described [e.g., *Day et al.*, 1999b]. Nevertheless, it can be appreciated (Figure 2) that for a few sites, mainly along the northern line (NL), and for high frequencies, the strike angle points towards a SE-NW direction. We interpret this as indicative of electric fields being deflected by shallow dike intrusions. *Day et al.* [1999b] suggest that the development of en echelon vent structures on the western flank of the Cumbre Vieja is caused by the decoupling of the deep triple-rift stress field from a near surface stress field dominated by the topographical-gravitational stresses. Other studies on the effect of topography on dike propagation have shown that dikes will propagate perpendicular to the direction of maximum tensile stress [*Cotterell and Rice*, 1980], and in the direction that will give the greatest normal stress at the tip of the dike. The greatest normal stress will be achieved by having a larger load on the surface which gives off a larger compressive stress [*Takada*, 1989].

[9] Figure 3 shows the strike angle that best fits a 2D model, independently of frequency, for sites *x*12 and *x*08. It can be observed that for site *x*12, at high frequencies the strike switches direction from a local SW-NE, dike driven direction to a regional N-S at lower frequencies (deeper structures); for site *x*08 the strike angle switches from a SE-NW angle at high frequencies, to a N-S at lower fre-

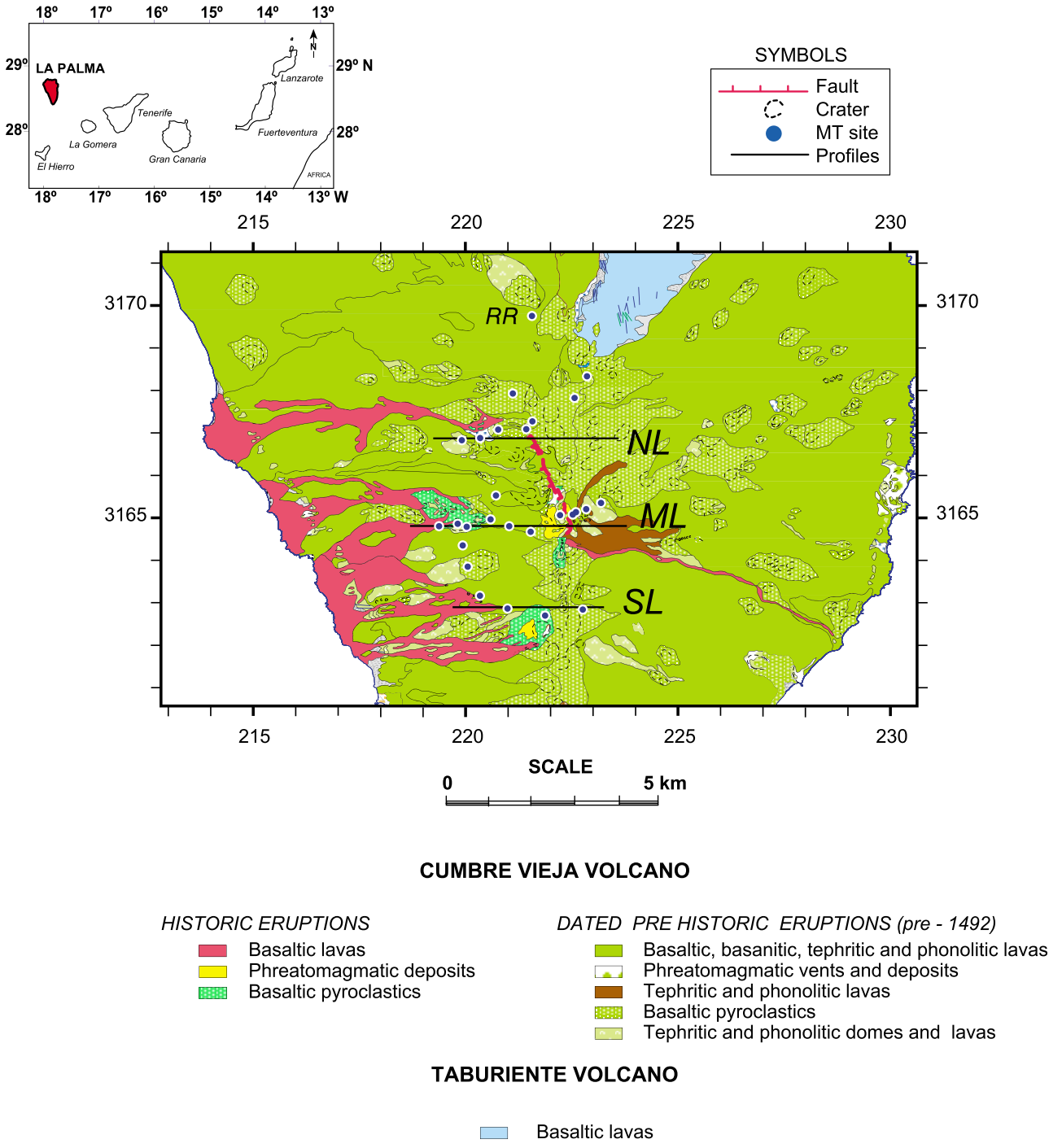

Figure 1. Geological map of La Palma. Blue dots: AMT sites. Black lines: profiles. Northernmost site is remote reference.

quencies, although there is no information about the presence or the surface expression of dikes at this location. In Figure 2 all the sites in which we have observed this behavior are marked with black dots.

[10] We have performed some 3D modeling to study the effects of these dikes. Appendix (A) shows the main results from our findings.

[11] An ideal approach at this stage would have been to undertake a full 3D inversion of the La Palma AMT data although the topography and the presence of the Ocean, with steep bathymetry yields this task impossible with today's computer capabilities. On the other hand, 2D inversion has been proven to be a good tool in volcanic environments [*Aizawa et al.*, 2009]. One of the advantages of the "strike" algorithm of *McNeice and Jones* [2001] is that it can calculate the best strike angle for a group of sites and frequencies. In our case, an angle of 4.5° W is the strike angle that best fits a 2D assumption for all frequencies and sites in

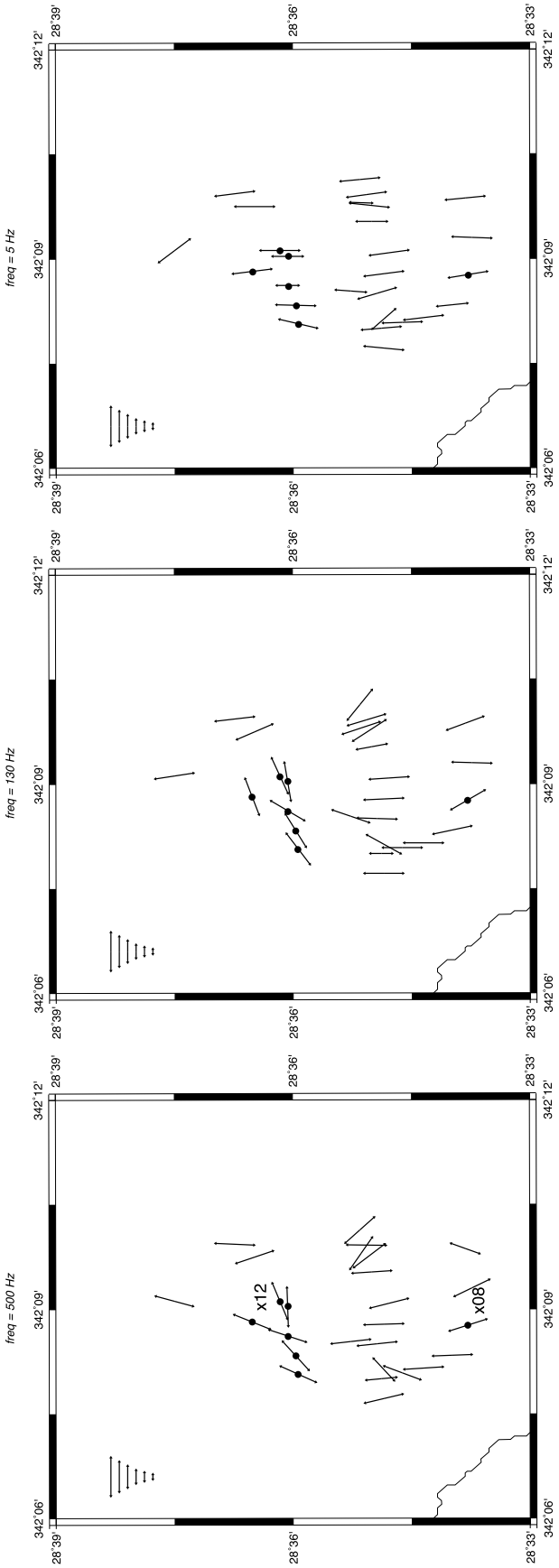

Figure 2. Map of electrical strike at 3 frequencies (500 Hz, 130 Hz and 5 Hz). Black dots indicate the position of those sites displaying a change in strike direction with depth. Strike angles for sites *x*12 and *x*08 are shown in more detail in Figure 3. The arrows on the top left corner indicate the RMS fit of the decomposition; from longer to shorter arrows: $RMS \leq 1$, $1 < RMS \leq 2$, $2 < RMS \leq 3$, $3 < RMS \leq 4$, $4 < RMS \leq 5$ and $RMS > 5$.

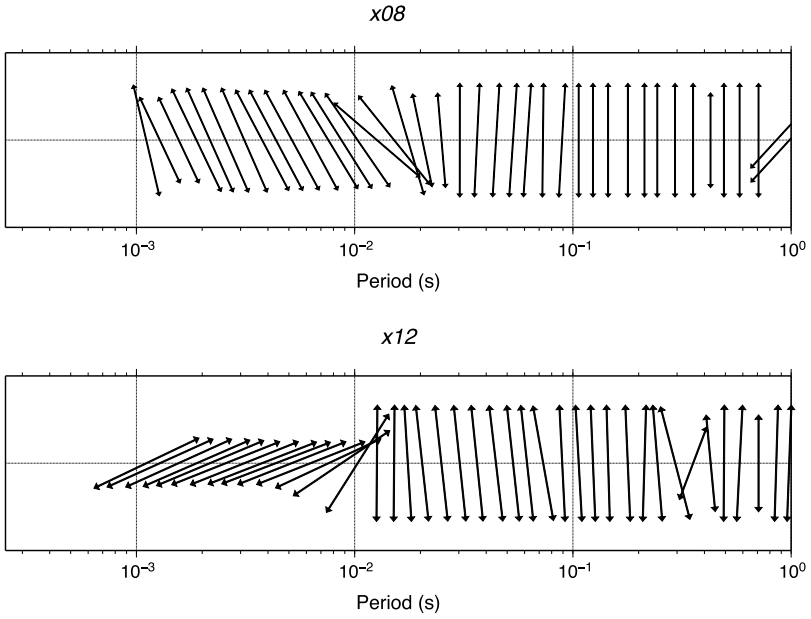

Figure 3. Frequency-dependent strike angle from sites $x12$ and $x08$ showing the change in strike direction coincident with the rotation of dikes on Cumbre Vieja. The particular strike angle of the vents near site $x12$ has been described by *Day et al.* [1999a].

each of the three profiles of our data set. We have also tested an angle of 0° obtaining a misfit that is similar to the best angle, therefore we opted for not rotating the data, thus avoiding mixing noise from different channels.

[12] Once the responses have been corrected for galvanic distortion and derived in the correct strike angle, they were inverted using the 2D inversion code of *Rodi and Mackie* [2001] as implemented in Geosystem's Winglink package, as this algorithm allows for inclusion of topography and bathymetry in the model. In our case we used the GEBCO 2003 and the ETOPO30 databases. We found that for the overall goals of this project, these topographic databases were satisfactory, and higher resolution would only be necessary for shallower studies. The sea layer has been fixed at $0.3\Omega \cdot m$. Fixing the sea layer has to be done with care as this conductive layer can cause anomalous conductive artifacts. We found that the inversion procedure produced conductive artifacts and also a conductive structure that "connects" the sea layer with the main conductive structure of the island. The next step was to include a resistive seafloor layer, but the inversion program could not fit the data satisfactorily and a large anomalous conductive structure appeared under the profile. Like *Unsworth et al.* [2007] we opted for using a "soft" constraint for the seafloor and Ocean layers. This technique allows the inversion code to relax the effect of the sea and fit the data.

[13] Since the strike analysis demonstrated these data could be interpreted using a 2D regional structure, we proceeded with the joint inversion of both (TE and TM) modes. The TE mode assumes that the electric current flows in the direction of the electric strike, while the TM mode assumes that the magnetic currents flow across the electric strike [*d'Erceville and Kunetz*, 1962]. To overcome potential problems with the regularization of the inversion procedure, this is initiated from a halfspace model of 1,000 Ω m of resistivity that includes topography and bathymetry, fixing the smoothing parameter (τ) to a particular value. This τ parameter controls the fitting of the data and the regularization of the resistivity model. For large values of τ the fit of the data worsens at the expense of making the model smoother. A good compromise is reached using what is called an "L"-shape curve [*Farquharson and Oldenburg*, 2004]. This curve can be obtained through a series of inversions using different τ parameters, plotting the final fit versus this smoothing τ parameter and thus defining the optimum model that fits the data with a reasonable smoothing. The optimum τ value obtained for the three profiles inverted in this work was 10. The fit of the data can be measured by the root-mean-square. Using an error floor of 10% on the apparent resistivities and 5% on the phases (in this program the phase error floor is entered as equivalent apparent resistivity percent, 5% is equivalent to 1.45 degrees) we reach a final RMS of 1.45, 1.53 and 1.36 for profiles NL, ML and SL. Apparent resistivity and phase pseudosections of the observed and modeled data are shown in Figure 4. As can be appreciated the fit is good, with the largest misfit being at the higher frequencies, probably caused by local 3D geology and rough topography. The inversion procedure also recovered the values of the static shifts at each site. As a reminder, these values were the only unknown parameter during the dimensionality and galvanic distortion analysis. We also undertook some inversions using a different background resistivity value for the starting model obtaining very similar final models and fits. A detailed explanation of the inversion process is given by *Unsworth et al.* [2007] and by *Spratt et al.* [2009].

[14] The three best-fitting models corresponding to the three profiles are shown in Figure 5. The horizontal black

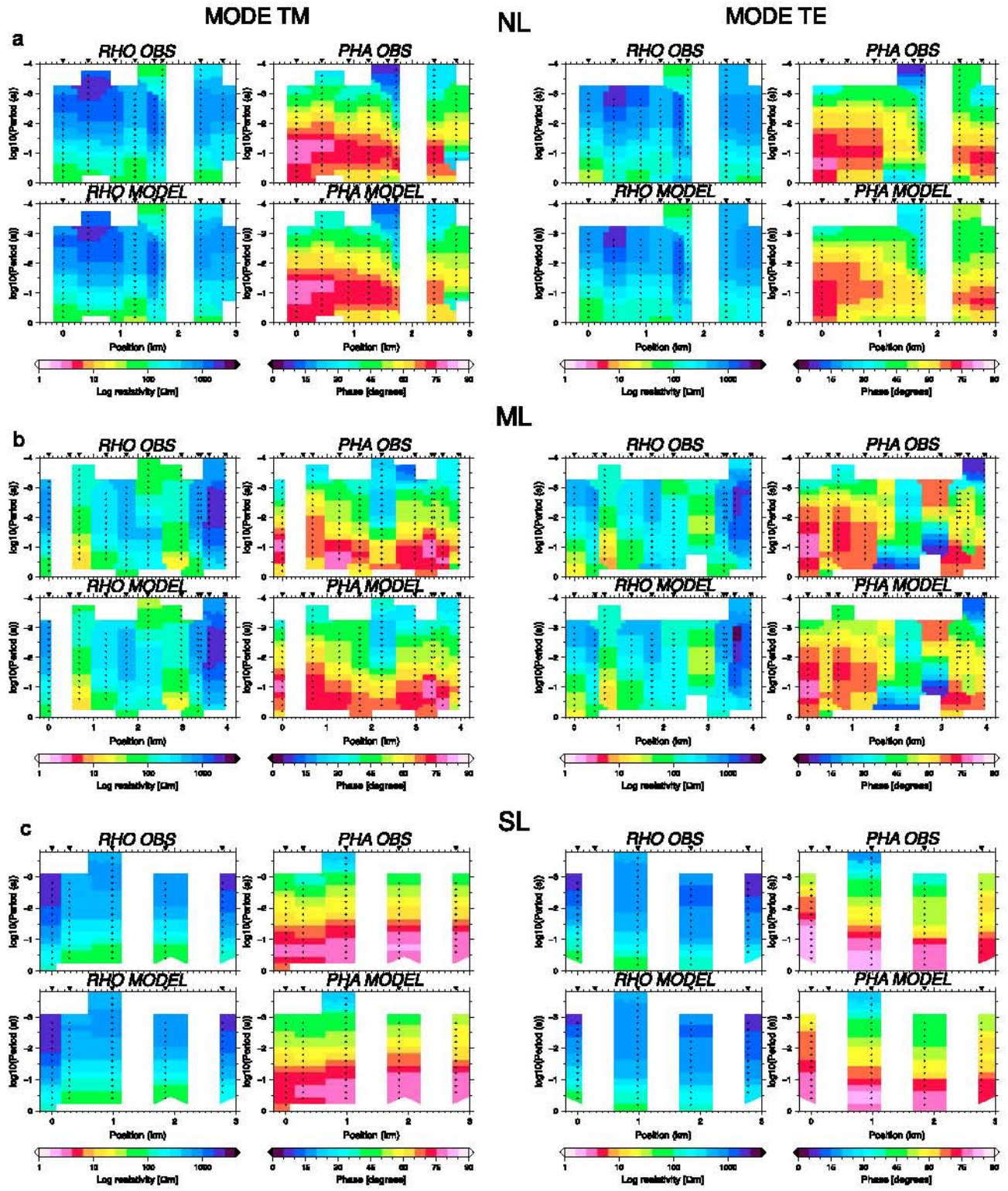

Figure 4. Pseudosections of observed and modeled apparent resistivities and phases for the three profiles used in this study. (a) Northern profile (NL). (b) Central profile (ML). (c) Southern profile (SL).

lines in the plots indicate the penetration depth for each site at the maximum period used in the 2D inversion, calculated using the Schmucker depth [*Schmucker*, 1970; *Jones*, 2006; *Spratt et al.*, 2009]. This function allows to obtain an approximate depth for which the attenuation of the wave is 1/2. These penetration depths are a guide to sensitivity to structure, as structures deeper than a poorly-penetrating site will be sensed by neighboring sites.

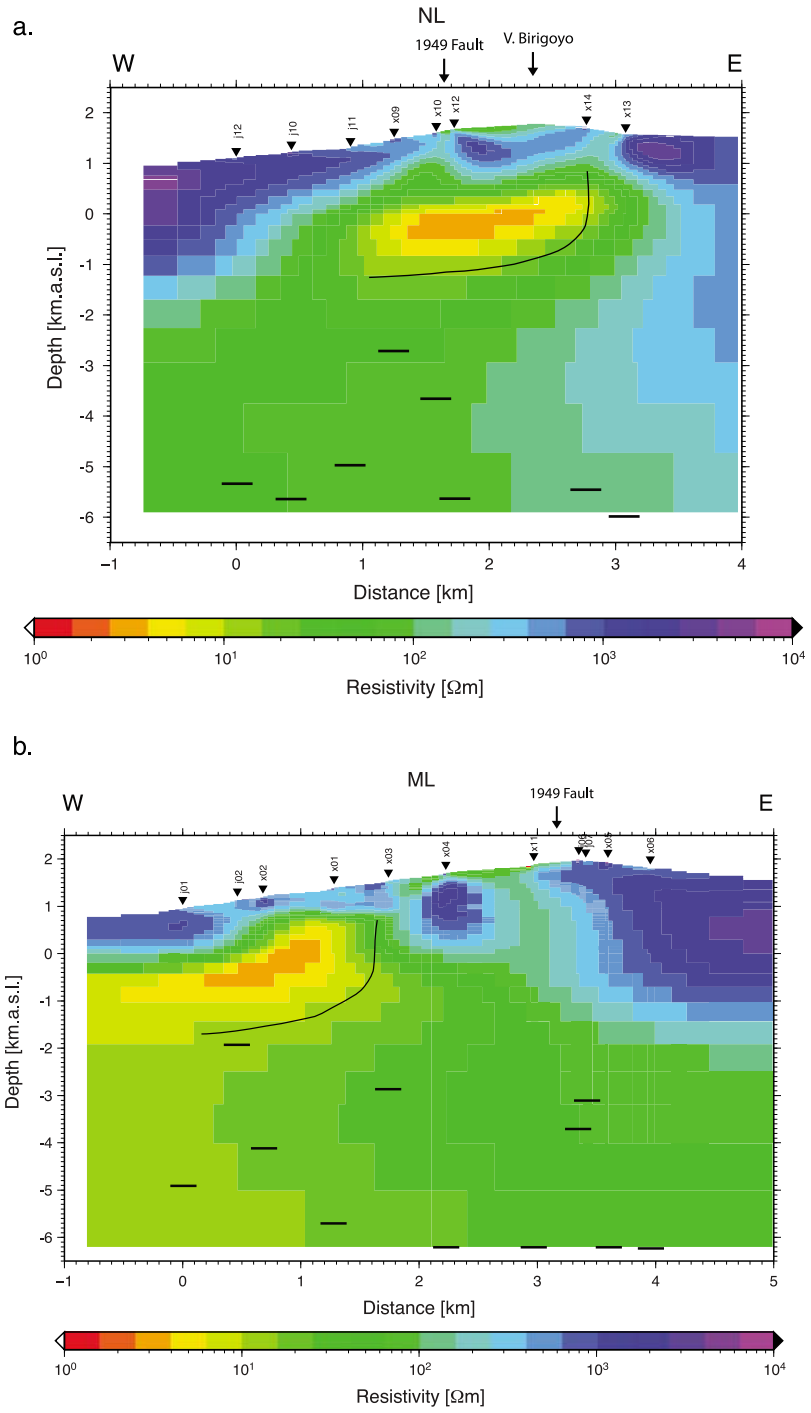

Figure 5. Two dimensional models corresponding to the three profiles realized on the Cumbre Vieja volcano western flank. The black lines underneath each site indicate the penetration depth calculated using the Niblett-Bostick transformation at the maximum period used for the 2D inversion. (a) Northern profile (NL). (b) Central profile (ML). (c) Southern profile (SL).

[15] The three profiles show similar resistivity structure with a top resistive layer overlying a more conductive area. The southern profile (SL) shows a more compact, resistive structure broken by a central conductive anomaly. The two other profiles show some breaks in the shallow resistive unit. On line NL one top layer break between sites *x*10 and *x*12, is spatially coincidental with the fault system developed during the 1949 eruption (see Figure 1 for detailed surface geology). On line ML, the top resistive layer is thinner and the break in the top resistive layer by site *x*11 is coincidental with the location of vents and craters of the 1585 eruption on the western flank of the island [*Carracedo et al.*, 2001].

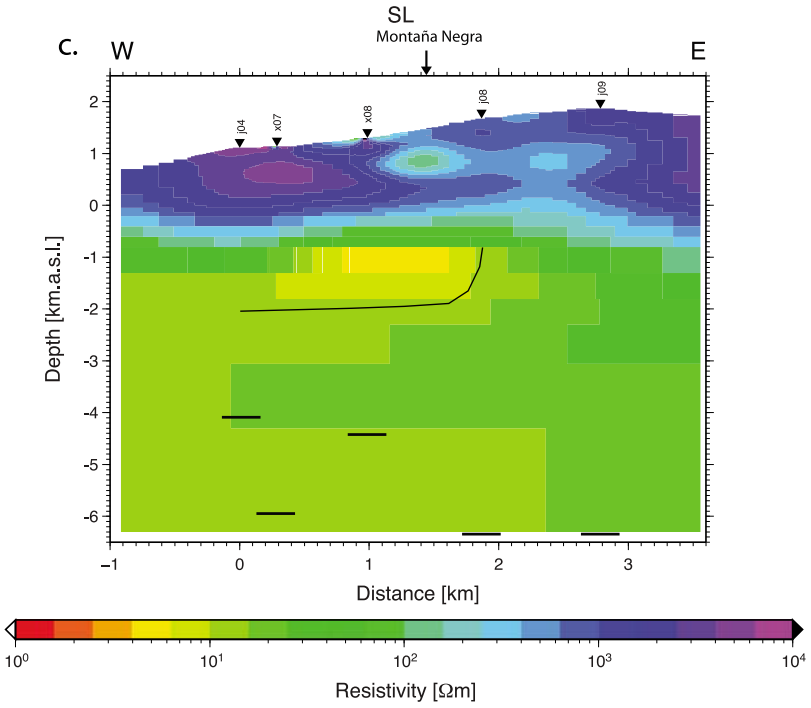

Figure 5. (continued)

The thickness of this top layer along profiles ML and NL is approximately 1 km, as suggested by the work of *Day et al.* [1999b]. This top resistive layer overlays a more conductive area on profiles ML and NL. According to geological models this could be an indication of either the presence of fluids or an alteration zone, and both of these interpretations require a zone of high porosity, like collapse debris material or hyaloclastites below the young Cumbre Vieja units. The resistivity models also show a resistive structure underneath this conductive anomaly, although because we restricted our field work to AMT frequencies the models cannot image in detail any deeper structures, but we interpret this as the old Cumbre Nueva basement. The other unique feature seen in profiles NL and ML is the resistive structure to the east of the profiles. This is a robust feature and any attempt to remove it from the models increases the misfit significantly. Also note the low conductive structure associated with the Birigoyo crater (Figure 5a), which is composed of basaltic, basanitic and tephritic pyroclasts, very loose material that allows for high porosities, thus explaining this conductive anomaly.

[16] Line SL shows a different behavior from profiles NL and ML (Figure 5c). On this profile we find that the top resistive structure of the island is thicker than to the north, and only a sub-horizontal elongated weak conductive anomaly at some 500 m depth beneath the Montaña Negra crater, that consists of pyroclastics. For this reason we think this enhanced conductivity is caused by the presence of saline water. At 1 km below sea level there is a conductive anomaly that correlates well with the anomalies observed on profiles NL (Figure 5a) and ML (Figure 5b). The main difference is that on this line the anomaly is sub-horizontal and there is no resistive anomaly to the east of the profile.

[17] As a test of reliability of the inversion models, we have also created a set of 2D inversions for line NS in which we only considered at each site the range of frequencies that correspond to a NS strike. These tests have started from the same halfspace model considered previously. The resulting inversion models (not shown here) show less control over the structures on the surface not affecting the regional structure that has been considered in this manuscript.

3. Discussion

[18] The present results show that the western flank of the Cumbre Vieja volcano consists of a 1 km thick resistive structure overlaying a more conductive structure. Similar conductive structures have been observed in the flanks of the Teide volcano in Tenerife, and have been interpreted as alteration zones composed of plastic breccia within a clayish matrix, developed over remnants of previous collapses [*Coppo et al.*, 2007]. *Ogawa et al.* [1998], using AMT data, showed that the Usu volcano (Hokaido, Japan) is underlain by a conductor interpreted as a geothermal water-bearing layer, although the top of this conductor consists of smectite, an alteration clay. This clay layer, besides being highly conductive, is impermeable, trapping fluids underneath that also increase conductivity. Similarly, *Schnegg* [1997] interpreted a conductive anomaly on the southern flank of the volcanic island of the Piton de la Fournaise (Reunion Island) as a clay bearing layer separating older units from more recent, and *Jones and Dumas* [1993] interpreted the presence

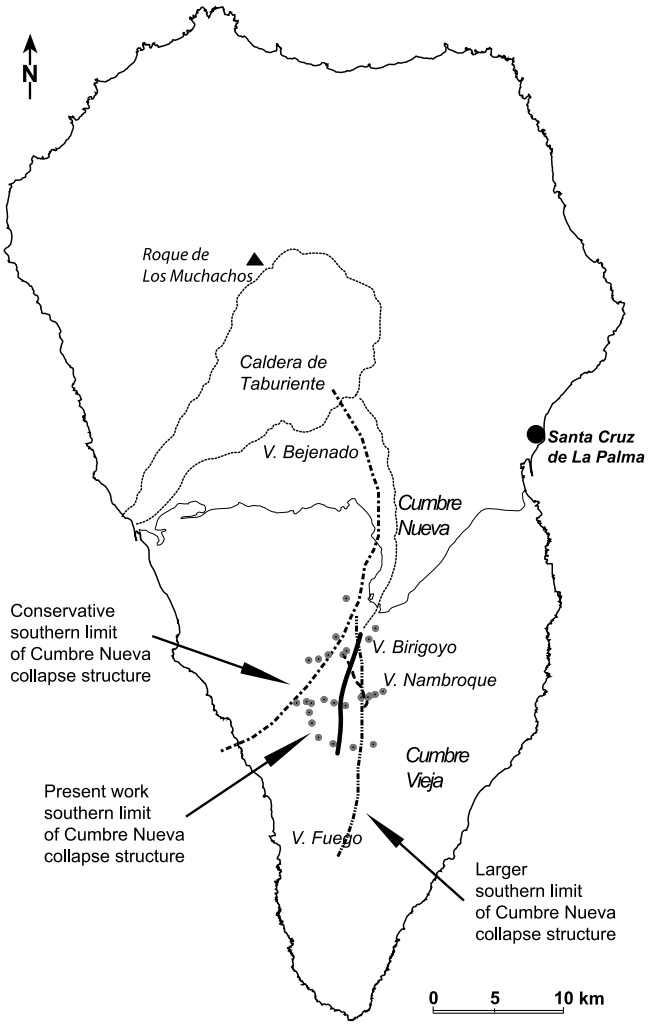

Figure 6. Map of the island of La Palma showing the position of the Cumbre Nueva units under the Cumbre Vieja volcano. The gray dots indicate the position of the AMT measurements. Solid line shows the scar inferred from the present work. Dashed-dotted lines show the inferred extension of these units from previous studies. Dotted lines show exposed collapse scars on the island.

of a clay layer beneath a Cascades volcano in British Columbia, Canada.

[19] Water, both fresh and sea water, is usually the fluid responsible for resistivity anomalies at depths considered in this study. On the island of La Palma, fresh water is extracted in the mountain for human use [*Carracedo et al.*, 2001], although it has been suggested that sea water flows towards the island [*Urgeles et al.*, 2000] and saline water intrusion has been reported in aquifers [*Consejo Insular de Aguas de La Palma*, 2001] close to shore. Nevertheless, the wells used for human consumption on the location of the profiles excludes the presence of sea water intrusion into the aquifers, and therefore we should rule out this possibility. Using Archie's law to obtain an approximate porosity for resistivities of 3–5$\Omega \cdot m$ [e.g., *Unsworth et al.*, 2007] we obtain porosities of the order of 40–50% for fresh water and porosities between 15–23% for sea water (being the upper and lower limits depending on the use of the cementation factor $m = 1$ for water distributed in cracks or $m = 1.5$ for well-connected pores). High porosities (40%) have been found in hyaloclastites [*Schiffman et al.*, 2005], but those were poorly consolidated and on the submarine flank of Mauna Kea (Hawaii), presenting a higher degree of compactification at higher depths. At the depths that we are considering in the island of La Palma, 1 to 3 km below the surface, the estimated values of the porosities are anomalously high. The lower values of porosity estimated for sea water (15–23%) are similar to the ones found by *Unsworth et al.* [2007], and could explain the conductive anomalies in the island, but there is no evidence of its presence in the study area. Another phase is necessary to explain this conductivity enhancement. Alteration clay (smectite) has been proposed for other volcanic islands, specifically in the island of Tenerife. It is a good conductor [*Ogawa et al.*, 1998], and a situation similar to the one described by *Ogawa et al.* [1998] in Usu volcano is applicable to the La Palma case: a combination of fluids trapped in this very porous layer with an alteration zone caused by the presence of fluids.

[20] We therefore interpret the conductive structure in the western flank of Cumbre Vieja volcano as an indication of the presence of debris material from the collapse of the Cumbre Nueva volcano and the later emplacement of Cumbre Vieja hyaloclastites on top of them, as suggested by *Day et al.* [1999b]. This interpretation of a weak layer is also reinforced by the observed rotation of the dikes as they ascend to surface (Figures 2 and 3). It has been suggested that this rotation indicates the presence of a boundary zone between the triple-rift zone and the topographical-gravitational stress zone, that is structurally weak [*Day et al.*, 1999b].

[21] Further, the interpretation of InSAR ground deformation data from *Gonzalez et al.* [2008] suggests a subhorizontal fault system at 2–3 km depth that correlates well with the results from the present work. A recent gravity survey [*Camacho et al.*, 2009] on the island of La Palma shows areas of low-density material on the western flank of the island, that have been interpreted as debris material from the collapse of the Cumbre Nueva volcano.

[22] There is a third possible cause of conductivity enhancement, namely partial melting, that we need to consider. If we track the conductive anomaly from the NL profile to the SL profile, and also consider the location of the fault system that developed during the 1949 eruption on profile NL, we see that the conductivity anomaly migrates west, and also from a depth of 1 km b.s.l. on profile ML to a depth of 1.5 km b.s.l. on profile ML and 2 km b.s.l. on profile SL. This structure is too large to be caused by a shallow magma chamber. Besides, temperatures of 650° C at 1–2 km below the surface would make the surface too hot to walk on! Therefore, we can reject this hypothesis.

[23] Using this conductive anomaly we can map the electrical expression of the footwall of the Cumbre Nueva units (Figure 6). In Figure 6 we have delimited the inferred unstable block using the results from the present work and we also show limits suggested by previous studies. Our proposed extension is situated between the more conservative model suggested by *Ancochea et al.* [1994] and *Carracedo* [1994], and the model suggesting a larger block of *Day et al.* [1999b].

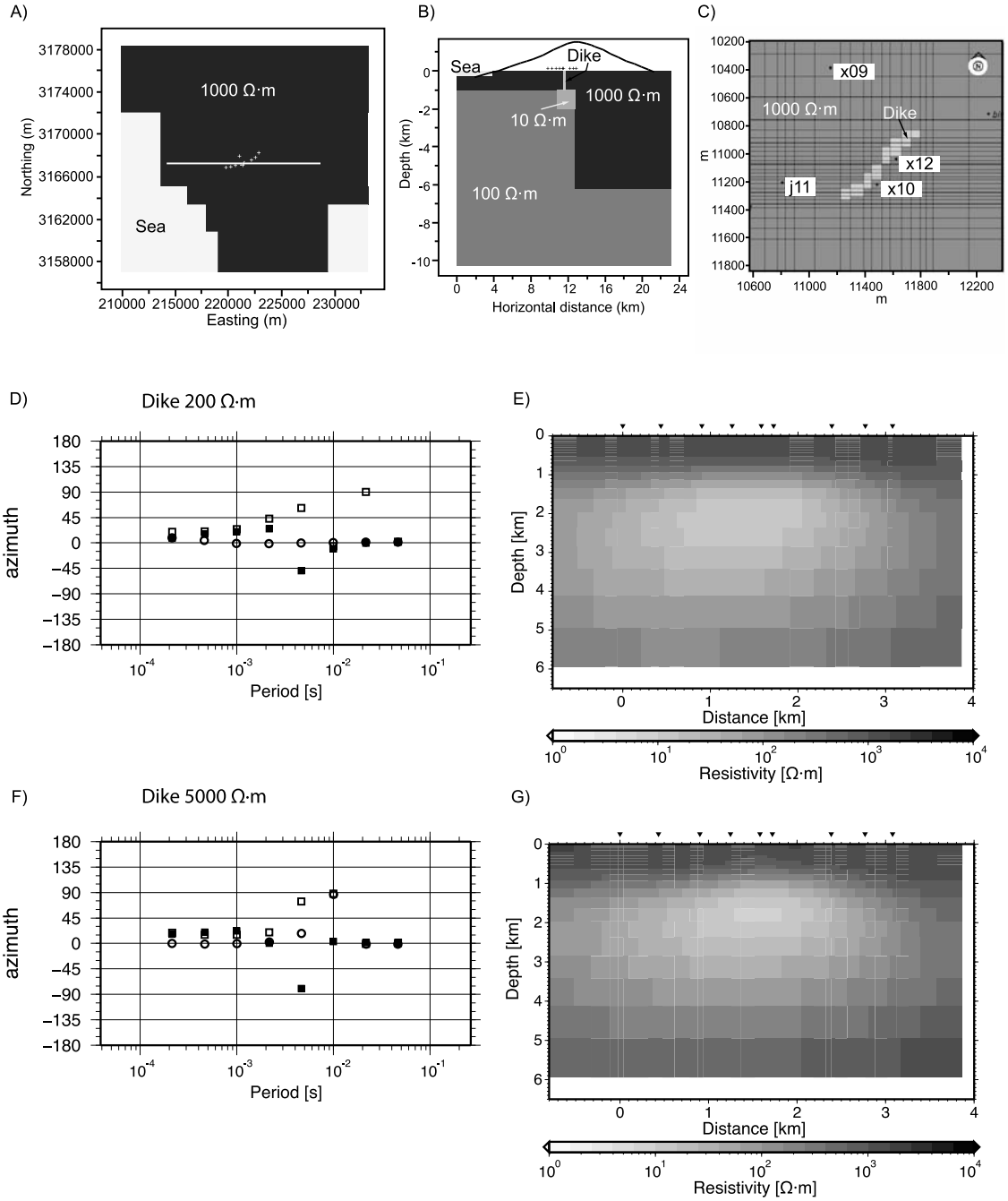

Figure A1. Results of 3D modeling of dike intrusions on profile NL. (a) Top view of the model (z = 0) showing station locations (crosses). (b) EW cut across 3D model showing station locations (crosses). The profile used in the 2D inversion is coincidental with this cut. The topography of the island is also included. (c) Detailed view of the dike intrusion (z = 0). (d) Strike angle for sites *x*12 (solid square), *x*10 (square) and *j*11 (circle) for a conductive dike intrusion ($200\Omega \cdot m$). (e) 2D inversion model across EW profile (Figure A1b) for a conductive dike. (f) Strike angle for sites *x*12 (solid square), *x*10 (square) and *j*11 (circle) for a resistive dike intrusion ($5000\Omega \cdot m$). (g) 2D inversion model across EW profile (Figure A1b) for a resistive dike.

[24] The resistive anomalies that we observe on the western end of profiles NL and ML (Figures 5a and 5b) probably indicate the presence of the feeding dikes for Cumbre Vieja volcano, as usually these are low porosity, highly resistive structures [*Ogawa et al.*, 1998]. Their contacts are usually marked by conductive anomalies caused by the presence of fluids, which is not the case on the western flank of the island of La Palma. More measure-

ments of the eastern part of the island are needed to properly map these possible anomalies.

4. Conclusions

[25] This work presents for the first time a electromagnetic study of the subsurface of the island of La Palma. The knowledge of the internal structure is key to study the evolution and also the potential hazards associated with weak zones. The present work maps the structures under the modern volcanic units of the Cumbre Vieja volcano, showing an area of enhanced conductivity interpreted as an alteration zone that also contains fluids.

[26] It has been suggested that the western flank of the island could potentially collapse and cause a tsunami of devastating consequences [*Ward and Day*, 2001; *Løvholt et al.*, 2008]. These two studies used the inferred geological model of the island of *Day et al.* [1999b], with a large western block collapsing towards the sea. In the present work we show that part of the southern extent of this western flank is close to the more conservative assumptions of *Ancochea et al.* [1994] and *Carracedo* [1994]. Based on the present work, future models of potential collapse of the western flank of the island will have to use the more conservative assumptions.

[27] The rotation of the dikes caused by the change of stress regime has also been imaged in the present work using an algorithm used in MT methods regularly to analyze dimensionality. The analysis shows a shallow direction of the dikes pointing in an approximated NE-SW direction and rotates gently towards a NS direction with depth. This result also suggests the existence of an structurally weak area at depths in which we locate the conductive anomaly. The ability of the MT method to detect these structures is discussed in Appendix A.

[28] To map properly the internal structure of the Cumbre Vieja volcano, more measurements have to be undertaken on the island, extending existing lines to the east and adding more profiles north and south of the present ones. Although, a fine 3D modeling with detailed topography and bathymetry of the island would be necessary to study the deeper structures of the island of La Palma [e.g., *Franke et al.*, 2007].

Appendix A: Strike Analysis of Synthetic 3D Models Including Dikes

[29] In this section we describe a modeling exercise to test the effect of dikes on the strike analysis and 2D inversion models, using a crude model of the island of La Palma. Note that none of the models that are described in this section include topography because of the amount of detail required, although the sea layer (bathymetry) has been included. To simplify the models even more only sites from the Northern Line (NL) have been considered as they are the ones affected by the emplacement of dikes (Figure 2). For the 3D forward modeling we have used the *Mackie et al.* [1994] MTD3FWD code implemented in Geosystem's Winglink package.

[30] In the first place we need to assess the effect of the surrounding sea on our data. To do this we construct a coarse homogeneous model of the island and test whether the sea affects the responses at the frequencies of interest. The results (not shown here) are that except for the western and southeastern margins of the island, closer to profile NL there is no noticeable sea effect at the frequencies of interest. Therefore we can simplify the model as it does not require as much bathymetric detail.

[31] The background model of the island is a simplified model from the 2D inversion of profile NL (Figure 5a). This model consists of a top 1 km resistive ($1{,}000\Omega \cdot m$) layer, overlying a vertical contact. Figure A1 shows an EW cut, top view (Figure A1b) and a detailed image from the dike (Figure A1c) of the model considered here. On the western part of the island we have reduced the conductivity to $100\Omega \cdot m$. Over the eastern part of the island, the top conductive structure has been extended down to 6 km depth. Below this 6 km a basal $100\Omega \cdot m$ layer has been placed. A 1 km thick conductive $10\Omega \cdot m$ structure, coincidental with the alteration layer, has also been placed in the model.

[32] As stated earlier, given the complexity of the study area the problem needs to be reduced and therefore we have considered only dikes under sites $x12$ and $x10$ (Figure A1c). We have tested different angles, but here we present results from the most representative, that corresponds to an strike angle of ~45° for the dikes. As dikes are basically basaltic structures they should be resistive, but the contact area with the host rock can be altered and therefore we consider two different situations. In the first one, dikes are considered as relatively conductive structures ($200\Omega \cdot m$); in the second one, as resistive ($5000\Omega \cdot m$) with respect to the resistivities of the host rock.

[33] In the first example the dikes are more conductive than the host rock ($200\Omega \cdot m$). In Figure A1d are shown the strike angle for two sites close to the dike, $x12$ (solid squares) and $x10$ (square) and for a site ~1 km away from the dike system $j11$ (circle). As can be appreciated the strike angle indicates the presence of a local structure for the sites next to the dike while the strike angle for site $j11$ is coincidental with the regional strike angle. The 2D inversion model is found in Figure A1e, showing a smoothed version of the regional model (Figure A1b) with no trace of anomalies caused by the dike on the surface. The data fit is acceptable with a final RMS of 1.5.

[34] Figures A1f and A1g show the example for a resistive dike ($5000\Omega \cdot m$). The strike analysis (Figure A1f) shows that the best strike angle that would explain the data from the two sites next to the dike, $x12$ (solid square) and $x10$ (square), deviates from the regional 0° angle. While site $j11$, ~1 km away from the dike, has a regional strike angle of 0° and thus is not affected by the local structure. The 2D inversion model (Figure A1g) also recovers the regional background resistivity (Figure A1b) and shows no trace of the dikes on the top layer.

[35] Both these examples, provide evidence that the inclusion of small scale, elongated structures on the uppermost layer of the crust can modify the strike angle of the MT responses, but it may be not imagined by the conductivity structure obtained from inversion. They also show that a site ~1 km away from the dike can be unaffected by it.

[36] **Acknowledgments.** The field work would not have been possible without the enthusiastic help of Jessica Spratt, Colin Hogg and Jan Schmoldt. We also thank the Environment Unit of the Cabildo de La Palma and the park rangers of the Natural Park of the Cumbre Vieja. Some plots have been generated using the GMT package [*Wessel and Smith*, 1998].

References

Aizawa, K., Y. Ogawa, and T. Ishido (2009), Groundwater flow and hydrothermal systems within volcanic edifices: Delineation by electric self-potential and magnetotellurics, *J. Geophys. Res.*, *114*, B01208, doi:10.1029/2008JB005910.

Ancochea, E., F. Hernán, A. Cendrero, J.-M. Cantagrel, J. Fúster, E. Ibarrola, and J. Coello (1994), Constructive and destructive episodes in the building of a young oceanic island, La Palma, Canary Islands, and the genesis of the Caldera de Taburiente, *J. Volcanol. Geotherm. Res.*, *60*, 243–262.

Bartel, L. C., and R. D. Jacobson (1987), Results of a controlled-source audiofrequency magnetotelluric survey at the Puhimau thermal area, Kilauea Volcano, Hawaii, *Geophysics*, *52*, 665–677.

Camacho, A. G., J. Fernández, P. J. González, J. B. Rundle, J. F. Prieto, and A. Arjona (2009), Structural results for La Palma island using 3-D gravity inversion, *J. Geophys. Res.*, *114*, B05411, doi:10.1029/2008JB005628.

Carracedo, J. C. (1994), The Canary islands: An example of structural control on the growth of large oceanic-island volcanoes, *J. Volcanol. Geotherm. Res.*, *60*, 225–241.

Carracedo, J. C., E. R. Badiola, H. Guillou, J. de la Nuez, and F. J. Pérez Torrado (2001), Geology and volcanology of La Palma and El Hierro, western Canaries, *Estud. Geol.*, *57*(5–6), 175–273.

Consejo Insular de Aguas de La Palma (2001), Plan hidrológico insular, *Bol. Off. Canarias*, *141*, 16,231–16,557.

Coppo, N., P.-A. Schnegg, P. Falco, and R. Costa (2007), Tsunamigenic risk for North Atlantic shorelines, in *Earth: Our Changing Planet: IUGG XXIV General Assembly, Perugia, Italy*, p. 1743, Umbria Sci. Meet. Assoc., Perugia, Italy.

Coppo, N., P.-A. Schnegg, P. Falco, R. Costa, and M. Burkhard (2008), Structural pattern of the western Las Cañadas caldera (Tenerife, Canary Islands) revealed by audiomagnetotellurics, *Swiss J. Geosci.*, *101*(2), 409–413, doi:10.1007/s00015-008-1270-4.

Cotterell, B., and J. Rice (1980), Slightly curved or kinked cracks, *Int. J. Fract.*, *16*(2), 155–169.

Day, S., S. H. da Silva, and J. Fonseca (1999a), A past giant lateral collapse and present day flank instability of Fogo, Cape Verde Islands, *J. Volcanol. Geotherm. Res.*, *94*, 191–218.

Day, S. J., J. Carracedo, H. Guillou, and P. Gravestock (1999b), Recent structural evolution of the Cumbre Vieja volcano, La Palma, Canary Islands: Volcanic rift zone reconfiguration as a precursor to volcano flank instability?, *J. Volcanol. Geotherm. Res.*, *94*, 135–167.

d'Erceville, E. J., and G. Kunetz (1962), The effect of a fault on the Earth's natural electromagnetic field, *Geophysics*, *27*, 651–665.

Farquharson, C. G., and D. W. Oldenburg (2004), A comparison of automatic techniques for estimating the regularization parameter in non-linear inverse problems, *Geophys. J. Int.*, *156*(3), 411–425, doi:10.1111/j.1365-246X.2004.02190.x.

Franke, A., S. Kütter, R.-U. Börner, and K. Spitzer (2007), Numerical simulation of magnetotelluric fields at stromboli, paper presented at 4th International Symposium on Three-Dimensional Electromagnetics, Inst. of Geophys., Tech. Univ. Bergakad. Freiberg, Freiberg, Germany.

Garcia, X., and A. G. Jones (2002), Atmospheric sources for audio-magnetotelluric (AMT) sounding, *Geophysics*, *67*, 448–458.

Garcia, X., and A. G. Jones (2008), Robust processing of magnetotelluric data in the AMT dead-band using the Continuous Wavelet Transform, *Geophysics*, *73*(6), F223–F234, doi:10.1190/1.2987375.

Gonzalez, P., J. Fernandez, A. Camacho, and K. Tiampo (2008), A slippery mechanical boundary at the western flank of Cumbre Vieja volcano, *Geophys. Res. Abstr.*, *10*, EGU2008-A-10432.

Groom, R. W., and R. C. Bailey (1989), Decomposition of magnetotelluric impedance tensors in the presence of local three-dimensional galvanic distorion, *J. Geophys. Res.*, *94*, 1913–1925.

Jones, A. G. (2006), Electromagnetic interrogation of the anisotropic Earth: Looking into the Earth with polarized spectacles, *Phys. Earth Planet. Inter.*, *158*(2–4), 281–291, doi:10.1016/j.pepi.2006.03.026.

Jones, A. G., and I. Dumas (1993), Electromagnetic images of a volcanic zone, *Phys. Earth Planet. Inter.*, *81*, 289–314.

Jones, A., A. Chave, G. Egbert, D. Auld, and K. Bahr (1989), A comparison of techniques for magnetotelluric response function estimation, *J. Geophys. Res.*, *94*, 14,201–14,213.

Krastel, S., H.-U. Schmincke, C. L. Jacobs, R. Rihm, T. P. L. Bas, and B. Alibés (2001), Submarine landslides around the Canary Islands, *J. Geophys. Res.*, *106*, 3977–3997.

Labazuy, P. (1996), Recurrent landslide events on the submarine flank of Piton de la Fournaise volcano (Reunion Island), in *Volcano Instability on the Earth and Other Planets*, edited by W. J. McGuire et al., *Geol. Soc. London Spec. Publ.*, *110*, 295–306.

Lipman, P., W. Normark, J. Moore, J. Wilson, and C. Gutmacher (1988), The giant submarine Alika Debris Slide, Mauna Loa, Hawaii, *J. Geophys. Res.*, *93*(B5), 4279–4299.

Løvholt, F., G. Pedersen, and G. Gisler (2008), Oceanic propagation of a potential tsunami from the La Palma Island, *J. Geophys. Res.*, *113*, C09026, doi:10.1029/2007JC004603.

Mackie, R. L., J. T. Smith, and T. R. Madden (1994), Three-dimensional electromagnetic modeling using finite difference equations: The magnetotelluric example, *Radio Sci.*, *29*(4), 923–935.

Manzella, A., and A. Zaja (2006), Volcanid structure of the southern sector of Mt. Etna after the 2001 and 2002 eruptions defined by magnetotelluric measurements, *Bull. Volcanol.*, *69*, 41–50.

Masson, D. G., A. Watts, M. Gee, R. Urgeles, N. Mitchell, T. L. Bas, and M. Canals (2002), Slope failures on the flanks of the Canary Islands, *Earth Sci. Rev.*, *57*, 1–35.

Matsushima, N., H. Oshima, Y. Ogawa, S. Takakura, H. Satoh, M. Utsugi, and Y. Nishida (2001), Magma prospecting in Usu volcano, Hokkaido, Japan, using magnetotelluric soundings, *J. Volcanol. Geotherm. Res.*, *109*, 263–277.

McNeice, G. W., and A. G. Jones (2001), Multisite, multifrequency tensor decomposition of magnetotelluric data, *Geophysics*, *66*, 158–173.

Mitchell, N. C., D. Masson, A. Watts, M. Gee, and R. Urgeles (2002), The morphology of the submarine flanks of volcanic ocean islands. A comparative study of the Canary and Hawaiian hotspot islands, *J. Volcanol. Geotherm. Res.*, *115*(1–2), 83–107, doi:10.1016/S0377-0273(01)00310-9.

Moore, J. G., D. Clague, R. Holcomb, P. Lipman, W. Normark, and M. Torresan (1989), Prodigious submarine landslides on the Hawaiian ridge, *J. Geophys. Res.*, *94*(B12), 17,465–17,484.

Moore, J. G., W. Bryan, M. Beeson, and W. Normark (1995), Giant blocks in the South Kona landslide, Hawaii, *Geology*, *23*(2), 125–128.

Moss, J. L., W. McGuire, and D. Page (1999), Ground deformation monitoring of a potential landslide at La Palma, Canary Island, *J. Volcanol. Geotherm. Res.*, *94*(1–4), 251–260, doi:10.1016/S0377-0273(99)00106-7.

Ogawa, Y., N. Matsushima, H. Oshima, S. Takakura, M. Utsugi, K. Hirano, M. Igarashi, and T. Doi (1998), A resistivity cross-section of Usu volcano, Hokkaido, Japan, by audiomagnetotelluric soundings, *Earth Planets Space*, *50*, 339–346.

Pous, J., W. Heise, P.-A. Schnegg, G. Muñoz, J. Martí, and C. Soriano (2002), Magnetotelluric study of the Las Cañadas caldera (Tenerife, Canary Islands): Structural and hydrogeological implications, *Earth Planet. Sci. Lett.*, *204*(1–2), 249–263, doi:10.1016/S0012-821X(02)00956-1.

Rodi, W., and R. L. Mackie (2001), Nonlinear conjugate gradients algorithm for 2-D magnetotelluric inversion, *Geophysics*, *66*, 174–187.

Schiffman, P., R. J. Watters, N. Thompson, and A. W. Walton (2005), Hyaloclastites and the slope stability of Hawaiian volcanoes: Insights from the Hawaiian Scientific Drilling Project's 3-km drill core, *J. Volcanol. Geotherm. Res.*, *151*(1–3), 217–228, doi:10.1016/j.jvolgeores.2005.07.030.

Schmucker, U. (1970), Anomalies of geomagnetic variations in the southwestern United States, *Bull. Scripps Inst. Oceanogr.*, *13*, 1–165.

Schnegg, P.-A. (1997), Electrical structure of Plaine des Sables caldera, Piton de la Fournaise volcano (Reunion Island), *Ann. Geophys.*, *XL*, 305–317.

Spratt, J. E., A. G. Jones, V. A. Jackson, L. Collins, and A. Avdeeva (2009), Lithospheric geometry of the Wopmay orogen from a Slave craton to Bear Province magnetotelluric transect, *J. Geophys. Res.*, *114*, B01101, doi:10.1029/2007JB005326.

Takada, A. (1989), Magma transport and reservoir formation by a system of propagating cracks, *Bull. Volcanol.*, *52*(2), 118–126.

Unsworth, M., W. Soyer, V. Tuncer, A. Wagner, and D. Barnes (2007), Hydrogeologic assessment of the Amchitka Island nuclear test site (Alaska) with magnetotellurics, *Geophysics*, *72*(3), B47–B57, doi:10.1190/1.2539353.

Urgeles, R., M. Canals, and J. Roberts (2000), Fluid flow from pore pressure measurements off La Palma, Canary Islands, *J. Volcanol. Geotherm. Res.*, *101*(3–4), 253–271, doi:10.1016/S0377-0273(00)00176-1.

Ward, S., and S. Day (2001), Cumbre Vieja Volcano—Potential collapse and tsunami at La Palma, Canary Islands, *Geophys. Res. Lett.*, *28*, 3397–3400.

Wessel, P., and W. H. F. Smith (1998), New, improved version of the Generic Mapping Tools released, *Eos Trans. AGU*, *79*, 579.

X. Garcia, Unitat de Tecnologia Marina, CSIC, Passeig Marítim de la Barceloneta 37-49, E-08003 Barcelona, Spain. (xgarcia@cmima.csic.es)

A. G. Jones, Geophysics Section, School of Cosmic Physics, Dublin Institute for Advanced Studies, 5 Merrion Square, Dublin 2, Ireland. (alan@cp.dias.ie)